JPE 16-5-22

http://dx.doi.org/10.6113/JPE.2016.16.5.1833
ISSN(Print): 1598-2092 / ISSN(Online): 2093-4718

Voltage Feedforward Control with Time-Delay Compensation for Grid-Connected Converters

Shude Yang† and Xiangqian Tong*

†,*School of Automation and Information Engineering, Xi'an University of Technology, Xi'an, China

Abstract

In grid-connected converter control, grid voltage feedforward is usually introduced to suppress the influence of grid voltage distortion on the converter's grid-side AC current. However, owing to the time-delay in control systems, the suppression effect of the grid voltage distortion is seriously affected. In this paper, the positive effects of the grid voltage feedforward control are analyzed in detail, and the time-delay caused by the low-pass filter (LPF) in the voltage filtering circuits and digital control are summarized. In order to reduce the time-delay effect on the performance of the feedforward control, a voltage feedforward control strategy with time-delay compensation is proposed, in which, a leading correction of the feedforward voltage is used. The optimal leading step used in this strategy is derived from analyzing the phase-frequency characteristics of a LPF and the implementation of digital control. By using the optimal leading step, the delay in the feedforward path can be further counteracted so that the performance of the feedforward control in terms of suppressing the influence of grid voltage distortion on the converter output current can be improved. The validity of the proposed method is verified through simulation and experiment results.

Key words: Feedforward control, Grid-connected converter, Leading correction, Time delay, Voltage distortion

I. INTRODUCTION

With the rapid development of new energy and smart grids, stringent requirements for power quality have been put forward in recent years. The static var generator (SVG), which is based on the voltage source converter, and the active power filter (APF), which is based on PWM control technology, provide reliable solutions for the improvement of power quality. The quality of the grid-side current is an important factor for measuring the performance of a converter, and Ref. [1] gives the limit of the harmonic current injected into the grid by converters. In reality, the performance of converter current control can be affected by non-ideal factors, such as the dead-time effect, the turn-on-off delay time, the conduction voltage drop across the power switches, etc. [2], [3]. It is also worth noting that grid background harmonics can also have a significant effect on the grid-side current quality [4]. In the worst case, they may cause a failure of the converter output current to satisfy the relevant standards [5], [6].

Manuscript received Mar. 3, 2016; accepted May 29, 2016
Recommended for publication by Associate Editor Hao Ma.
†Corresponding Author: yangshude858755@163.com
Tel: +86-029-82312002, Xi'an University of Technology
*School of Automation and Information Engineering, Xi'an University of Technology, China

For the grid-side current control, the grid background harmonics can be regarded as a disturbance in the current control loop. According to control theory, improving the open-loop gain at the harmonic frequencies can suppress the effect of a distorted grid voltage on the grid-side current. However, increases in the open-loop gain are restricted by the system stability. A proportional resonance (PR) regulator provides a greater gain only at selected resonant frequencies. Therefore, it can work well in suppressing grid-voltage harmonics with the resonant frequency of the PR. Multiple paralleled PR regulators can be adopted to suppress the influence of harmonic voltages on output currents with different orders [7]. However, this decreases the system stability margin. Thus, corresponding phase compensation methods have to be utilized to overcome this problem. However, this increases the difficulty of the control system design [8], [9]. In [10], proportional integral (PI) controllers in multiple synchronous frames were adopted to suppress the grid-voltage harmonics. However, multiple complex coordinate transforms are involved in this method and their time consumption increases dramatically when more grid background harmonics need to be dealt with.

Another way to suppress grid-voltage distortion is to use grid-voltage feedforward control [11]-[13]. This can reduce the

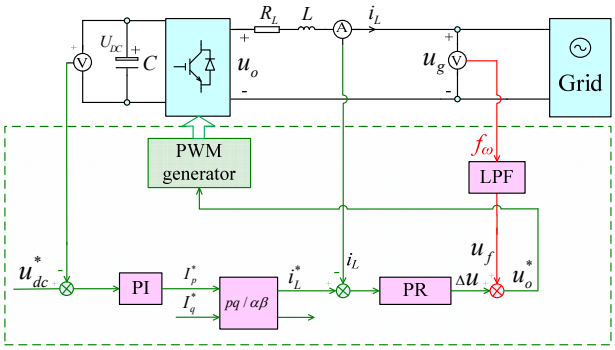

Fig. 1. Grid-connected converter system.

startup current of the device and improve the system dynamic performance [14], [15]. Unlike the multiple PR control, the grid-voltage feedforward has no influence on the stability margin of the system. As a result, it is widely used in grid-connected converter control. However, for the traditional feedforward control used in the above papers, the sampled grid-voltage is directly added into the current regulator output without consideration of nonlinear factors, such as the signal conditioning, PWM control and sampling. In fact, a low-pass filter (LPF) in the grid-voltage filtering circuit will produce different phase lags at different frequency components, and the PWM control and sampler will also cause some delays [16]-[19]. Both of them reduce the performance of the feedforward control in terms of suppressing grid background harmonics. A feedforward control with only one step prediction of the feedforward voltage is adopted in [20], and only the delay caused by the voltage filtering is considered in [21]. These factors limit the suppression ability in terms of grid background harmonics. In [22], a feedforward selective harmonics compensation method based on a band-pass filter (BPF) is proposed to compensate the delay caused by digital control. However, when the number of selective harmonics increases, a large number of BPFs are needed. Furthermore, the design method for the parameters of each BPF is complex. Compared with the traditional feedforward control, the full-feedforward schemes proposed in [23]-[25] can dramatically improve the suppression ability in terms of grid background harmonics. However, their algorithms are complex and contain the first-order and second-order derivative functions that amplify the high-frequency noise. This may affect the system performance and even endanger the safety of the device operation.

In this paper, the delay in the feedforward path caused by the LPF in voltage filtering circuits and digital control is carefully analyzed and a new feedforward control strategy with a leading correction of the feedforward voltage is proposed. This strategy dramatically improves the suppression ability of the converter on the grid-voltage distortion by compensating the delay in the feedforward path.

This paper is organized as follows. Section II introduces the principles and the positive effects of the grid-voltage feedforward control. The main factors causing delays in the control system are analyzed in Section III, including the LPF in the grid-voltage filtering circuits and the digital control. The proposed control scheme is presented in Section IV, and the design method of the optimal leading step used in the proposed scheme is also given. The effectiveness of the proposed scheme is verified by simulation and experiment results in Section V. Finally, Section VI concludes this paper.

II. Grid-Voltage Feedforward Control

A. Principle of Grid-Voltage Feedforward Control

The grid-side current control of a voltage source converter is realized by the control of the amplitude and phase of the converter output voltage at the AC side. The current is generated by this voltage and the grid voltage on the two terminals of the filter reactor. Therefore, the active and reactive components of the grid-side current can be controlled by regulating the converter output voltage. In addition, the DC voltage control can be realized by adjusting the active current.

Fig. 1 shows a schematic diagram of the *L*-filtered static var generator system used in this study. The active component reference of the grid-side current is the output of the DC voltage regulator in the form of PI, and the reactive component reference is obtained from the load current calculation or manual setting. Then the reference current in the natural coordinate can be determined by a coordinate transformation from the active and reactive components, and the converter output voltage is given by the current regulator output according to the error between the reference and the output current. Owing to the ability to track a sinusoidal reference with zero steady-state error, a PR regulator is used in the inner current loop for the fundamental output current control of the converter.

For a convenient analysis, the converter output voltage at the AC side can be divided into two components. One is the synchronous voltage, which has the same amplitude and phase as the grid voltage and generates zero grid-side current. The other is the voltage difference between the grid voltage and converter output voltage, which generates grid-side current through an *L*-filter. If the grid voltage feedforward is unused, i.e., the path denoted by f_ω in Fig. 1 is removed, both of the components are generated by the current regulator. However, if a grid voltage feedforward path exists, the current regulator only outputs the second component, which generates the grid-side current. Hence, the dynamic performance of the system can be remarkably improved as illustrated in the following subsections.

B. Improvement of the Startup Performance Owing to Grid-Voltage Feedforward Control

From the above analysis, the current regulator must generate a synchronous voltage component to counteract the influence of the grid voltage on the converter output current when the

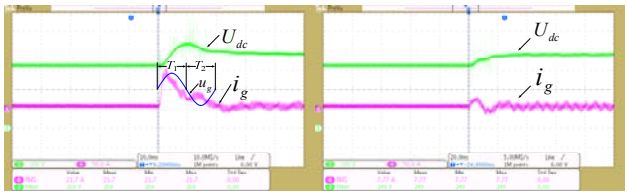

(a) (b)

Fig. 2. Experiment results of the startup performance. (a) Without grid-voltage feedforward control. (b) With grid-voltage feedforward control.

grid voltage feedforward is not adopted. In the startup stage of the converter, it takes some time for the current regulator to generate this component. Therefore, a current shock and a DC voltage overshoot usually occur, as shown in Fig. 2(a), where i_g, u_g and U_{dc} are the grid current, the grid voltage in one cycle and the DC voltage, respectively. The grid voltage is positive in the time interval T_1, and the DC voltage is lower than its reference value at the beginning of the startup stage. As a result, a positive i_g is generated from the DC regulator to charge the capacitor, and an obvious voltage overshoot occurs near the end of T_1. Owing to this overshoot and the negative grid voltage during T_2, the DC voltage regulator still generates a positive i_g to discharge the capacitor to regulate the voltage towards its reference value.

When the feedforward control is adopted, the synchronous component is directly added into the output of the current regulator without the requirements of the regulating process. Accordingly, the shock in the startup stage can be greatly reduced and the DC voltage overshoot can be eliminated. With the same control parameters used in Fig. 2(a), the startup performance of the converter with the grid voltage feedforward control is shown in Fig. 2(b). It shows a prominent improvement.

C. The Suppression Ability of the Feedforward Control on the Influence of Grid-Voltage Distortion

Using Kirchoff's laws on the main circuit shown in Fig.1, a differential equation of the physical quantities can be given by:

$$u_o - u_g = R_L i_L + L\frac{di_L}{dt} \tag{1}$$

Using Laplace transformation, the converter output current can be expressed in the s-domain as:

$$I_L(s) = \frac{U_o(s) - U_g(s)}{R_L + Ls} \tag{2}$$

Based on (2), a control diagram of the grid-connected converter with the voltage feedforward control is shown in Fig. 3, where $G_F(s)$, $G_{\mathrm{PWM}}(s)$, $G_c(s)$ and $G_L(s)$ are the transfer functions of the LPF in the grid-voltage filtering circuit, the PWM control, the current regulator, and the L-filter. The path f in the figure is the grid-voltage feedforward path.

From (2), the transfer function of the L-filter can be written as:

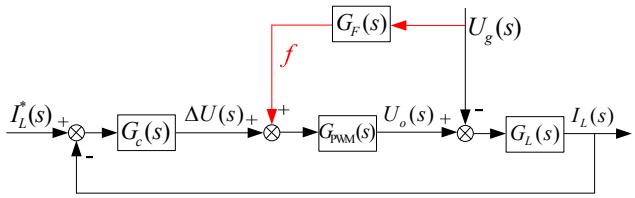

Fig. 3. Control diagram of the converter with grid-voltage feedforward.

$$G_L(s) = \frac{1}{R_L + Ls} \tag{3}$$

If a PR controller is used in the inner current loop, its transfer function can be expressed as [26]:

$$G_c(s) = K_p + \frac{2K_r\omega_c s}{s^2 + 2\omega_c s + \omega_0^2} \tag{4}$$

where, K_p is the proportional gain mainly affecting the response speed of the system, ω_0 is the resonant frequency, ω_c is the resonance bandwidth, and K_r is the resonance gain at the resonant frequency. In this study, K_p=2, K_r=80, ω_0=100π and ω_c=4π are used.

From Fig. 3, the relation between the grid voltage and the grid-side current can be given by:

$$\frac{I_L(s)}{U_g(s)} = \frac{G_F(s)G_{\mathrm{PWM}}(s) - 1}{1 + G_c(s)G_{\mathrm{PWM}}(s)G_L(s)} G_L(s) \tag{5}$$

In the ideal condition of $G_{\mathrm{PWM}}(s)$ =1 and $G_F(s)$ =1, the right-hand side term of the above equation is zero. That is, the influence of the grid background voltage harmonics on the converter's output current can be completely eliminated by the grid voltage feedforward control.

III. TIME DELAY CAUSED BY THE LPF AND DIGITAL CONTROL

The principle of the suppression of the grid-voltage distortion for the feedforward control is that the converter quickly outputs a voltage which is exactly equal to the distorted grid voltage. Therefore, the distorted grid voltage is completely counteracted by this voltage, and the influence of the grid voltage distortion on the grid-side current can be avoided. However, if a delay exists between the feedforward voltage and the real grid voltage, the compensation precision of the grid-voltage disturbances will be decreased, and the suppression ability of the feedforward control on harmonic voltages will be weakened.

The delay between the feedforward voltage and the real grid voltage may be caused by a large number of factors in practice. Among them, the LPF in the voltage filtering circuits and the digital control are two major factors.

A. Time Delay Caused by an Analog Filter

In the control system for a grid-connected converter, the

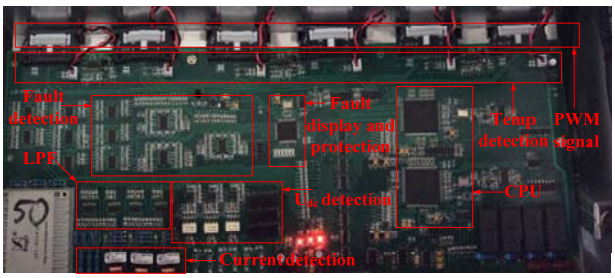

Fig. 4. Prototype of the control board for grid-connected converter.

LPF is usually designed to filter noise and to ensure the accuracy of the sampling signals. Fig.4 shows the control board used in the following experimental study. It contains current detection, temperature detection, LPF, fault detection, fault display and protection, CPU and PWM signals. The widely-used second-order LPF can be expressed as:

$$G_F(s)=\frac{1}{\frac{1}{\omega_{cf}^2}s^2+\frac{1}{Q\omega_{cf}}s+1} \tag{6}$$

where, ω_{cf} and Q are the cut-off frequency and quality factor of the LPF. The phase lag caused by the LPF at the frequency ω_f can be given by:

$$\varphi_{df}=\arctan(\frac{\omega_f\omega_{cf}}{Q(\omega_{cf}^2-\omega_f^2)}) \tag{7}$$

Due to the approximately linear phase-shift characteristics below the cut-off frequency, the phase lag caused by a LPF can be treated as a pure time delay. Taking the power frequency as an example, the delayed time can be expressed as:

$$T_{LPF}=\arctan(\frac{\omega_1\omega_{cf}}{Q(\omega_{cf}^2-\omega_1^2)})/\omega_1 \tag{8}$$

where, ω_1 is the power frequency. Therefore, below the cut-off frequency, the LPF can be expressed simply as:

$$G_F(s)\approx e^{-T_{LPF}s} \tag{9}$$

Both the frequency responses of the LPF described by (6) and the corresponding pure time delay function obtained from (9) are shown in Fig. 5 for comparison. Obviously, the LPF can be equivalent to a pure time delay function below the cut-off frequency.

B. Time Delay Caused by the Digital Control

With the rapid development of digital signal processing technology, digital control has become mainstream technology for grid-connected converters. Compared with analog control, digital control has higher reliability, is smaller in volume, lower in energy consumption and higher in flexibility. Largely owing to such advantages, it is convenient to realize complex and intelligent algorithms to achieve higher performance of converters. However, it also brings

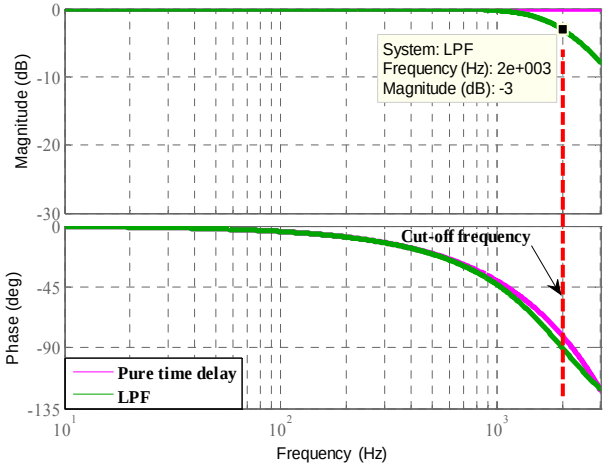

Fig. 5. Frequency responses of the LPF and corresponding pure time delay function.

some drawbacks. Just take the PWM technology widely used in converter control as an example. One of these drawbacks is the maximal duty-cycle limitation due to sampling and computation. As a result, the one-step-delay control method is usually used for the converter control. This produces some delays between the calculation of the output-voltage reference of the converter and the updating of the PWM comparison value [16]. The updating frequency is related to the loading mode of the PWM module in the digital signal processor (DSP). The PWM comparison value usually updates only at the peak or the trough of the carrier wave. That is to say, it updates once in a switching cycle. If it updates at the peak and the trough of the carrier wave, this is twice in a switching cycle. Whether it updates once or twice in a switching cycle, the delay always exists. The mechanism for the delay caused by the PWM updating is illustrated in Fig. 6 when the comparison value updates once in a switching cycle (only updated at the trough of the carrier wave).

Provided that the DSP is interrupted at n moment, the PWM comparison value corresponding to u_f(n-1)+Δu(n-1) and obtained in the previous period will be updated immediately (the meaning of the symbols u_f and Δu are shown in Fig. 1). In the present period, the grid voltage u_f(n) is sampled, and from Fig. 1, the output-voltage reference of the converter can be determined by the sum of u_f(n) and Δu(n). However, the corresponding PWM comparison value makes no contribution in the current switching cycle. It will not be loaded until the DSP is interrupted again in the next switching cycle. From the above, it is obvious that the loading mode of the PWM comparison value produces a switching cycle delay. Therefore, the delay caused by the PWM loading can be modeled as:

$$G_d(s)=e^{-T_s s} \tag{10}$$

where, T_s is the switching cycle. In addition, when the PWM comparison value is updated, this value is maintained

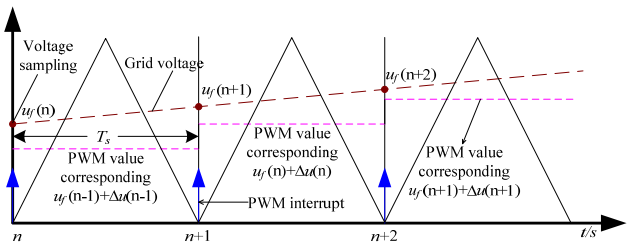

Fig. 6. The delay caused by PWM loading.

constantly until the next switching cycle. Then the duty cycle of the PWM wave is generated by a comparison between this value and the triangular carrier wave. This behavior can be modeled as a zero order holder (ZOH) [17], which can be expressed as $(1-e^{-T_s s})/s$. In view of the sampler represented by $1/T_s$, the delay caused by the ZOH and the sampler can be modeled as:

$$G_h(s)=\frac{1}{T_s}\cdot\frac{1-e^{-T_s s}}{s}\approx e^{-0.5T_s s} \tag{11}$$

The PWM comparison value is updated only at the trough of the carrier wave in the following study. In other words, it updates once in a switching cycle. Therefore, the total time delay caused by the digital control is about $1.5T_s$, which can be expressed as:

$$G_{\mathrm{PWM}}(s)=e^{-1.5T_s s} \tag{12}$$

From the above analysis, if a PWM comparison value updates twice in a switching cycle, the total time delay caused by the digital control will be about one switching cycle.

IV. Time-Delay Compensation for Grid-Voltage Feedforward Control

In order to analyze the time delay in the feedforward path, the control diagram shown in Fig. 3 is equivalently converted into Fig. 7(a). Obviously, the total delay between the feedforward voltage and the real grid voltage is the sum of the delay caused by the LPF and the digital control, which can be expressed as (13).

$$G_D(s)=G_{\mathrm{PWM}}(s)\cdot G_F(s)=e^{-mT_s s} \tag{13}$$

where, m is defined as the leading correction factor in the base of a switching cycle T_s. In view of the analyses in III.A and III.B and the PWM loading mode used in the following study, the value of m can be given by:

$$m=1.5+\frac{T_{LPF}}{T_s} \tag{14}$$

In order to compensate the delay in the feedforward path, a leading correction function $G_p(s)$ for the feedforward voltage is proposed to be embedded in the feedforward path as shown in Fig. 7(b). If the transfer function is selected as:

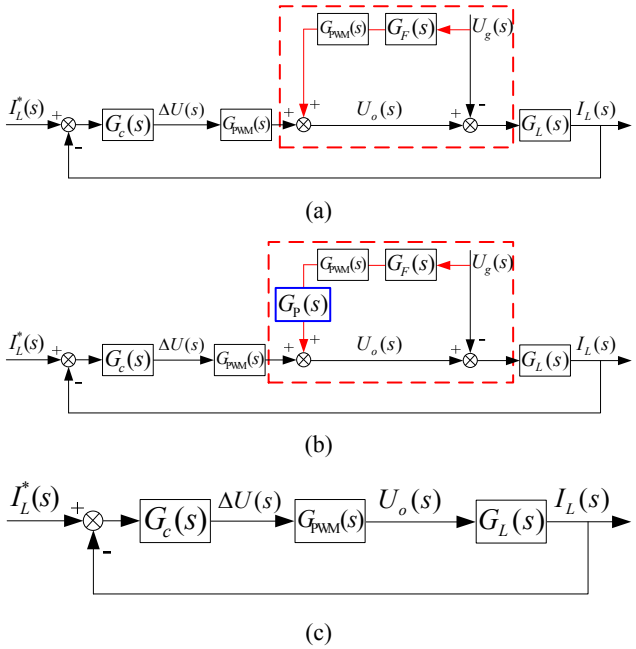

Fig. 7. Control diagram of the grid-connected converter. (a) Equivalent control diagram of Fig.3. (b) Delay compensation in the feedforward path. (c) Equivalent control diagram when the time delay is fully compensated.

$$G_{\mathrm{P}}(s)=1/G_D(s)=e^{mT_s s} \tag{15}$$

the delay in the feedforward path is fully compensated and the corresponding control diagram can be simplified as Fig. 7(c).

When the leading correction algorithm described by (15) can be realized with the leading correction factor obtained from (14), the delay in the feedforward path is fully compensated, and the grid-side current is not affected by grid voltage distortion. However, it should be noticed that the leading correction factor m should be an integer in practice due to the discreteness of the digital control period, while it is usually a decimal according to (14). The integer m is called the leading step in the following study. Since the AD conversion and the PWM reversal cannot be completed immediately, the optimal leading step should be the smallest integer that is greater than or equal to the number calculated from (14) in practice. Therefore, the optimal leading step should be selected as:

$$m=\left\lceil 1.5+\frac{T_{LPF}}{T_s}\right\rceil \tag{16}$$

If m has been selected as an integer according to (16) in the z domain, the leading correction algorithm with the optimal leading step described by (15) can be expressed as:

$$G_{\mathrm{P}}(z)=z^m \tag{17}$$

For a positive integer, (17) cannot be realized in a general control system. However, distorted grid voltages are usually periodic. Owing to the periodic recurrence characteristic of

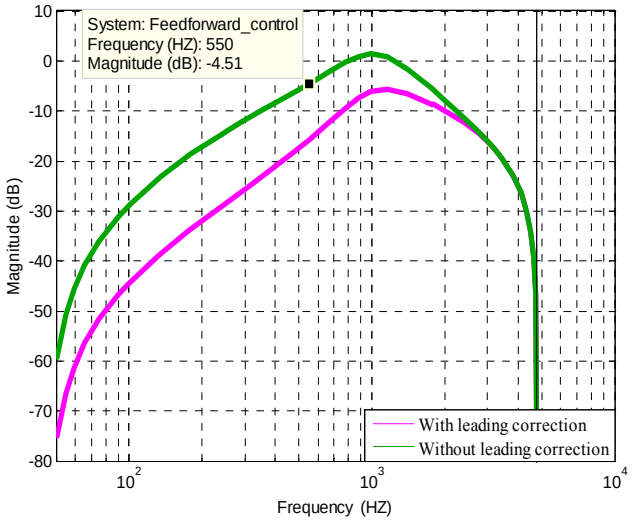

Fig. 8. Frequency responses of grid-side current versus grid voltage with feedforward control.

integer harmonics in grid voltage, the leading correction algorithm can be realized in series with a one-cycle delay module, which can be expressed as:

$$G_{\mathrm{P}}(z) = z^{-N} z^{m} = z^{-N+m} \tag{18}$$

where, N is the number of sampling points in a power cycle, which is set as 192 in the following study.

With consideration of the leading correction in the feedforward path in Fig. 7(b), the effect of grid voltage on the grid-side current can be expressed in the z-domain as:

$$\frac{I_L(z)}{U_g(z)} = \frac{G_{\mathrm{P}}(z)G_F(z)G_{\mathrm{PWM}}(z)-1}{1+G_c(z)G_{\mathrm{PWM}}(z)G_L(z)} G_L(z) \tag{19}$$

The cut-off frequency and quality factor used for the LPF are 2 kHz and 0.707 in the following study, which can be expressed as (6). In order to analyze the effect of grid voltage harmonics on the grid-side current in the z-domain, the First-Order Holder (FOH) [27] method is used here to obtain $G_c(z)$, $G_L(z)$, $G_{\mathrm{PWM}}(z)$ and $G_F(z)$ from the corresponding s-domain transfer functions, where, $G_{\mathrm{PWM}}(s)$ is approximately equivalent to a first-order process.

For the LPF and PWM loading mode used in this study, the optimal leading step m =3 can be obtained according to (8) and (16).

When the leading correction of the feedforward voltage is not used, $G_{\mathrm{p}}(z)$ =1 should be selected. Substituting discrete transfer functions into (19), the frequency responses of the grid-side current versus the grid voltage can be obtained. The amplitude-frequency characteristics at the integer harmonic frequencies both with and without the leading correction algorithm are shown in Fig. 8.

Fig. 8 shows that without the leading correction of the feedforward voltage, the amplitudes at lower integer frequencies such as the 3rd and 5th harmonics are relatively lower. However, the amplitude at the frequency of the 11th harmonic is only about -4.5dB, which reflects the low suppression ability on grid-voltage harmonic. Thus, it can be concluded that owing to the delay caused by the LPF and the digital control, the performance of the feedforward control on reducing the effect of the grid voltage harmonics on the grid-side current is poor, especially at the relatively higher harmonic frequencies. Even the harmonics near 1000 Hz will be enlarged. It also shows that the amplitude-frequency characteristics at integer harmonics shift down when the leading correction is adopted. This illustrates the improved suppression ability of the control system on grid voltage harmonics with the leading correction.

TABLE I
SYSTEM PARAMETERS

Symbol	Description	Value
U_{g}	Grid voltage (rms)	380 V
I_{o}	Rated current	100 A
f_{s}	Switching frequency	9.6 kHz
L	Filter inductance	0.25 mH
R_L	L-filter resistor	10 mΩ
C	DC capacitor	2820μF

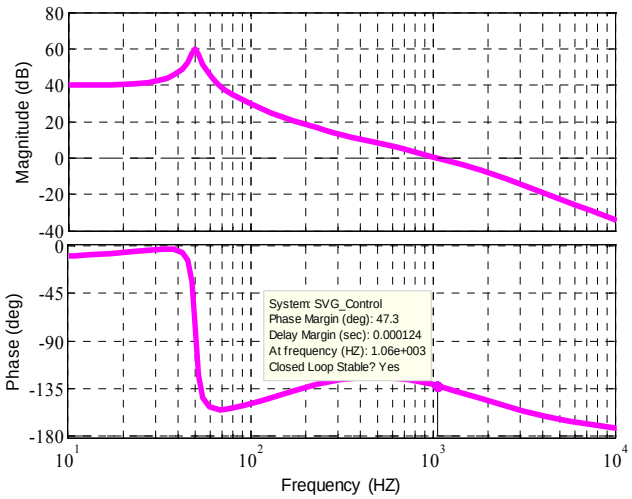

Fig. 9. Bode plots of the open-loop transfer function.

V. SIMULATION AND EXPERIMENT RESULTS

In order to verify the effectiveness of the proposed control strategy, some simulation and experimental results of the proposed control strategy are presented and compared. The main circuit and a control block diagram of the grid-connected converter used in the simulations and experiments are shown in Fig. 1. The main parameters for the system are shown in Table I.

With the abovementioned control parameters, bode plots of the open-loop transfer function are given in Fig. 9. The cross-over frequency is set as 1 kHz, which is about one-tenth of the switching frequency [28], and the phase margin is

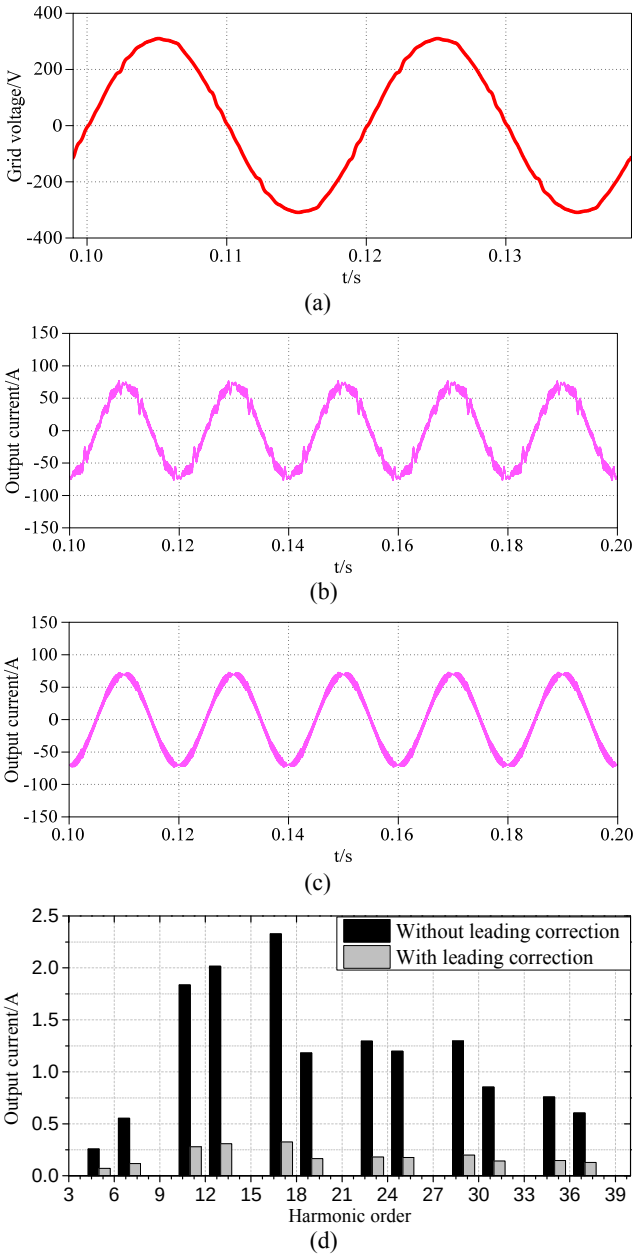

Fig. 10. Simulation results. (a) Distorted grid voltage. (b) Grid-side current for feedforward control without leading correction. (c) Grid-side current for feedforward control with leading correction. (d) Harmonic spectrum of the grid-side current.

about 47°. The gain at 50Hz is about 60dB, which guarantees the strong ability to track the power frequency signal.

A. Simulation Results

A simulation model is built in the Matlab/PLECS environment, and the control algorithm is realized in the S-Function. The PWM comparison value updates once a switching cycle for the simulations and experiments. The optimal leading step used in the following study is 3.

Fig. 10(a) shows the distorted grid voltage used for the simulation. The output current of the converter with or without the leading correction of the feedforward voltage is

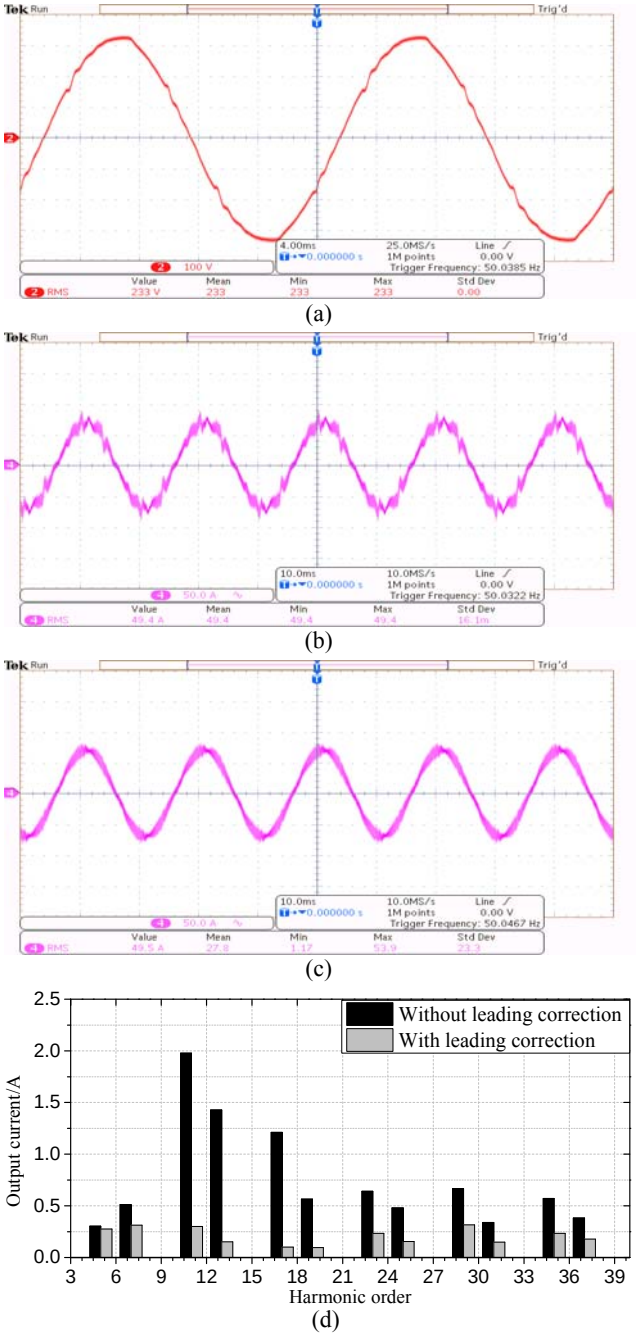

Fig.11. Experiment results. (a) Distorted grid voltage. (b) Grid-side current for feedforward control without leading correction. (c) Grid-side current for feedforward control with leading correction. (d) Harmonic spectrum of the grid-side current.

shown in Fig. 10(c) and (b) and their harmonic spectrums are given in Fig. 10(d) for a detailed comparison. Obviously, because of the delay in the feedforward path, the grid-side current is seriously affected by grid voltage harmonics when the leading correction is not adopted. However, this affection can be well suppressed by using the proposed leading correction scheme.

B. Experiment Results

The proposed scheme is also verified in a static var

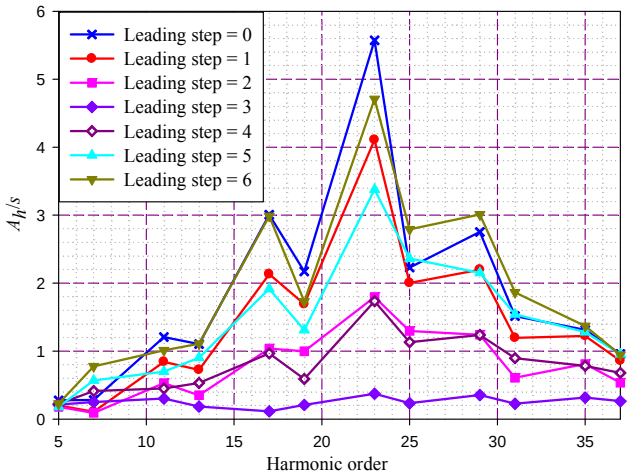

Fig. 12. Experiment admittance of the converter at different voltage harmonics with different leading steps.

generator prototype with a TMS320F28335 controller. Fig. 11(a) shows the grid voltage with the distortion used in the experiment, and the grid-side current for the feedforward control without the leading correction is shown in Fig. 11(b). It can be seen that the grid-side current contains harmonics caused by the grid voltage distortion, and that the total harmonic distortion (THD) of the grid-side current is about 8.08%.

With the same control parameters and experimental conditions, the grid-side current for the proposed scheme is shown in Fig. 11(c). In addition, Fig. 11(d) shows the harmonic spectrums of the output current of the converter with and without the proposed scheme. Obviously, owing to the leading correction of the feedforward voltage, the effect of the grid voltage harmonics is suppressed well, and the THD of the grid-side current is reduced from 8.08% to 2.23%.

There are some differences between the experimental and simulation results as shown in Fig. 10 and Fig. 11. These differences can be caused by the following factors. Normally variations do exist between the nominal and the real value of *L*-filters and the LPF used in the experiment and the inductances vary with the current level, so that the values are not constant during operation [29], [30]. All of them affect the suppression ability of the converter on grid-voltage distortions. In addition, some other factors cause harmonics in the grid-side current besides the grid voltage distortion, such as the dead-time that is injected into the PWM signals to avoid the shoot-through of the power switches in a converter leg.

In order to quantify the suppression ability of the converter on the h^{th} grid voltage harmonic, an equivalent admittance for the h^{th} harmonic is defined as:

$$A_h = \frac{I_h}{U_h} \tag{20}$$

where, A_h is the converter's equivalent admittance at the h^{th} harmonic frequency, and I_h and U_h are the h^{th} harmonic components in the grid-side current and voltage, respectively. A_h reflects the response of converter to grid voltage harmonics under different control strategies and parameters.

Fig. 12 shows some experiments results of the converter's equivalent admittance at different harmonic frequencies with different leading steps. It shows that a leading step of 3 is the optimum value, and that the greater the deviation of the leading step from this value is, the larger the admittance of the converter at harmonic frequencies becomes, or the larger the influence of the grid voltage distortion on the grid-side current becomes.

VI. Conclusions

Grid voltage feedforward control is an effective method for suppressing the influence of grid voltage distortion on converter output current and for attenuating starting currents. However, a delay in the feedforward path such as that from a LPF and digital control will weaken its suppression ability in terms of grid-voltage harmonics. By the above theoretical analysis, simulation and experiment results, it can be concluded that:

1) Both the LPF in the conditioning circuit for the grid voltage detection and the digital control will introduce some delay in the grid voltage feedforward path.

2) The delay in the feedforward path will cause an asynchrony between the feedforward voltage and the real grid voltage. This asynchrony reduces the performance of the feedforward control in terms of suppressing the influence of grid voltage distortion on converter output current.

3) A delay in the feedforward path can be compensated by introducing a leading correction function of the feedforward voltage. Owing to this strategy, the performance of the feedforward control can be markedly improved.

4) In digital control, an optimal leading step exists for a given LPF and PWM operation mode. In addition, the greater the deviation from this step is, the worse the feedforward performance becomes in terms of suppressing the influence of grid voltage distortion on the converter output current becomes.

Acknowledgment

This work was supported by the National Nature Science Foundation of China under grant 51507139, the Major Scientific and Technological Innovation Projects of Shaanxi Province under grant 2015ZKC02-01 and the Key Discipline Special Foundation of Shaanxi Province under Grant 5X1301.

References

[1] *IEEE Standard for Interconnecting Distributed Resources With Electric Power Systems*, IEEE Std. 1547-2003, Jul. 28, 2003.

[2] I. Dolguntseva, R. Krishna, D. E. Soman, and M. Leijon, "Contour-based dead-Time harmonic analysis in a three-level neutral-point-clamped inverter," *IEEE Trans. Ind. Electron*., Vol. 62, No. 1, pp. 203-210, Jun. 2015.

[3] D.-H. Lee and J.-W. Ahn, "A simple and direct dead-time effect compensation scheme in PWM-VSI," *IEEE Trans. Ind. Appl*., Vol. 50, No. 5, pp. 3017-3025, Sep. 2014.

[4] H. Zhou, Y. W. Li, N. R. Zargari, Z. Cheng, R. Ni, and Y. Zhang, "Selective harmonic compensation (SHC) PWM for grid-interfacing high-power converters," *IEEE Trans. Power Electron*., Vol. 29, No. 3, pp. 1118-1127, Mar. 2014.

[5] *IEEE Recommended Practices and Requirements for Harmonic Control in Electrical Power Systems*, IEEE Std. 519-1992, May 10, 1992.

[6] *IEEE Recommended Practice for Utility Interface of Photovoltaic (PV) Systems*, IEEE Std. 929-2000, Jan. 2000.

[7] Z. Li, Y. Li, P. Wang, H. Zhu, C. Liu, and F. Gao, "Single-loop digital control of high-power 400-Hz ground power unit for airplanes," *IEEE Trans. Ind. Electron*., Vol. 57, No. 2, pp. 532-543, Feb. 2010.

[8] L. F. A. Pereira, J. V. Flores, G. Bonan, D. F. Coutinho, and J. M. G. D. S. Jr, "Multiple resonant controllers for uninterruptible power supplies – A systematic robust control design approach," *IEEE Trans. Ind. Electron*., Vol. 61, No. 3, pp. 1528-1538, Mar. 2014.

[9] Y. Yang, K. Zhou, and M. Cheng, "Phase compensation resonant controller for PWM converters," *IEEE Trans. Ind. Informat*., Vol. 9, No. 2, pp. 957-964, May. 2013.

[10] P. Xiao, K. A. Corzine, and G. K. Venayagamoorthy, "Multiple reference frame-based control of three-phase PWM boost rectifiers under unbalanced and distorted input conditions," *IEEE Trans. Power Electron*., Vol. 23, No. 4, pp. 2006-1127, Jul. 2017.

[11] A. Luo, Y. Chen, Z. Shuai, and C. Tu, "An improved reactive current detection and power control method for single-phase photovoltaic grid-connected DG system,"*IEEE Trans. Energy. Convers*., Vol. 28, No. 4, pp. 823-831, Dec.2013.

[12] J. Kan, S. Xie, Y. Wu, Y. Tang, Z. Yao, and R. Chen, "Single-stage and boost-voltage grid-connected inverter for fuel-cell generation system," *IEEE Trans. Ind. Electron*., Vol. 62, No. 9, pp. 5480-5490, Sep. 2015.

[13] Y. Han, P. Shen, and J. M.Guerrero, "Stationary frame current control evaluations for three-phase grid-connected inverters with PVR-based active damped LCL filters," *Journal of Power Electronics*, Vol. 16, No. 1, pp. 297-309, Jan. 2016.

[14] D. Sun, B. Ge, W. Liang, H. Abu-Rub, and F. Z. Peng, "An energy stored quasi-Z-source cascade multilevel inverter-based photovoltaic power generation system," *IEEE Trans. Ind. Electron*., Vol. 62, No. 9, pp. 5458-5467, Sep. 2015.

[15] Y. Chen, A. Luo, Z. Shuai, and S. Xie, "Robust predictive dual-loop control strategy with reactive power compensation for single-phase grid-connected distributed generation system," *IET Power Electron*., Vol. 6, No. 7, pp. 1320-1328, Jan. 2013.

[16] Z. Wan, J. Xiong, J. Lei, C. Chen, and K. Zhang, "A modified capacitor current feedback active damping approach for grid connected converters with an LCL filter," *Journal of Power Electronics*, Vol. 15, No. 5, pp. 1286-1294, Sep. 2015.

[17] D. Yang, X. Ruan, and H. Wu, "A real-time computation method with dual sampling modes to improve the current control performances of the LCL-type grid-connected inverter," *IEEE Trans. Ind. Electron*., Vol. 62, No. 7, pp. 4563-4572, Jul. 2015.

[18] T.-L. Lee, Y.-C. Wang, J.-C. Li, and J. M. Guerrero, "Hybrid active filter with variable conductance for harmonic resonance suppression in industrial power systems," *IEEE Trans. Ind. Electron*., Vol. 62, No. 2, pp. 746-756, Feb. 2015.

[19] L. Harnefors, A. G. Yepes, A. Vidal, and J. Doval-Gandoy, "Passivity-based controller design of grid-connected VSCs for prevention of electrical resonance instability," *IEEE Trans. Ind. Electron*., Vol. 62, No. 2, pp. 702-710, Feb. 2015.

[20] J. R. Fischer, S. A. Gonzalez, M. A. Herran, M. G. Judewicz, and D. O. Carrica, "Calculation-delay tolerant predictive current controller for three-phase inverters," *IEEE Trans. Ind. Informat*., Vol. 10, No. 1, pp. 233-242, Feb. 2014.

[21] T.-V. Tran, T.-W. Chun, H.-H. Lee, H.-G. Kim, and E.-C. Nho, "Control method for reducing the THD of grid current of three-phase grid-connected inverters under distorted grid voltages," *Journal of Power Electronics*, Vol. 13, No. 4, pp. 712-718, Jul. 2013.

[22] X. Wu, X. Li, X. Yuan and Y. Geng, "Grid harmonics suppression scheme for LCL-type grid-Connected inverters based on output admittance revision," *IEEE Trans. Sustain Energy*., Vol. 6, No. 2, pp. 411-421, Aprial. 2015.

[23] M. Xue, Y. Zhang, Y. Kang, Y. Yi, S. Li, and F. Liu, "Full feedforward of grid voltage for discrete state feedback controlled grid-connected inverter with LCL filter," *IEEE Trans. Power Electron*., Vol. 27, No. 10, pp. 4234-4247, Oct. 2012.

[24] X. Wang, X. Ruan, S. Liu, and C. K. Tse, "Full feedforward of grid voltage for grid-connected inverter with LCL filter to suppress current distortion due to grid voltage harmonics," *IEEE Trans. Power Electron*., Vol. 25, No. 12, pp. 3119-3127, Dec.2010.

[25] W. Li, X. Ruan, D. Pan, and X. Wang, "Full-feedforward schemes of grid voltages for a three-phase LCL-type grid-connected inverter," *IEEE Trans. Ind. Electron*., Vol. 60, No. 6, pp. 2237-2250, Jun. 2013.

[26] D.-Y. Kim, W.-S. Im, S.-H. Hwang and J.-M. Kim, "Compensation of current offset error in half-bridge PWM inverter for linear compressor," *Journal of Power Electronics*, Vol. 15, No. 6, pp. 1593-1600, Nov. 2015.

[27] A. G. Yepes, F. D. Freijedo, J. Doval-Gandoy, O. Lo´pez,J. Malvar, and P. Fernandez-Comesa˜na, "Effects of discretization methods on the performance of resonant controllers," *IEEE Trans. Power Electron*., Vol. 25, No. 7, pp. 1692-1712, Jul.2010.

[28] R. W. Erickson and D. Maksimovic, *Fundamentals of Power Electronics*,2nd ed. Norwell, MA: Kluwer, pp.330-410, 2001.

[29] T.-F. Wu, C.-H. Chang, L.-C. Lin, Y.-C. Chang, and Y.-R. Chang, "Two-phase modulated digital control for three-phase bidirectional inverter with wide inductance variation," *IEEE Trans. Power Electron*., Vol. 28, No. 4, pp.1598-1607, April 2013.

[30] T.-F. Wu, C.-H. Chang, L.-C. Lin, G.-R. Yu, and Y.-R. Chang, "A D−Σ digital control for three-phase bidirectional inverter to achieve active and reactive power injection," *IEEE Trans. Ind. Electron*., vol. 61, no. 8, pp. 3879-3890, Aug. 2014.

Shude Yang was born in Henan, China, in 1986. He received his B.S. and M.S. degrees in Electrical Engineering from Henan Polytechnic University, Jiaozuo, China, in 2009 and 2012, respectively. Since 2012, he has been working towards his Ph.D. degree in the School of Automation and Information Engineering, Xi'an University of Technology, Xi'an, China. His current research interests include power quality, renewable energy generation, and the control and stability analysis of grid-connected converter systems.

Xiangqian Tong was born in Shaanxi, China, in 1961. He received his B.S. degree in Electrical Engineering from the Shaanxi Institute of Technology, Hanzhong, China, in 1983; his M.S. degree from the Xi'an University of Technology, Xi'an, China, in 1989, and his Ph.D. degree in Electrical Engineering from Xi'an Jiaotong University, Xi'an, China, in 2006. He joined the Xi'an University of Technology, in 1989. Since 2002, he has been a Professor and the Academic Leader of Electrical Engineering with the Xi'an University of Technology. His current research interests include the application of power electronics in power systems, and the control of power quality, especially power filters, static synchronous compensators, and high voltage direct current.